Ab initio Calculations of the Isotopic Dependence of Nuclear Clustering

Serdar Elhatisari,[1,2] Evgeny Epelbaum,[3,4] Hermann Krebs,[3,4] Timo A. Lähde,[5] Dean Lee,[6,7,4] Ning Li,[5] Bing-nan Lu,[5] Ulf-G. Meißner,[1,5,8] and Gautam Rupak[9]

[1]*Helmholtz-Institut für Strahlen- und Kernphysik and Bethe Center for Theoretical Physics, Universität Bonn, D-53115 Bonn, Germany*

[2]*Department of Physics, Karamanoglu Mehmetbey University, Karaman 70100, Turkey*

[3]*Institut für Theoretische Physik II, Ruhr-Universität Bochum, D-44870 Bochum, Germany*

[4]*Kavli Institute for Theoretical Physics, University of California, Santa Barbara, California 93106-4030, USA*

[5]*Institute for Advanced Simulation, Institut für Kernphysik, and Jülich Center for Hadron Physics, Forschungszentrum Jülich, D-52425 Jülich, Germany*

[6]*National Superconducting Cyclotron Laboratory, Michigan State University, East Lansing, Michigan 48824, USA*

[7]*Department of Physics, North Carolina State University, Raleigh, North Carolina 27695, USA*

[8]*JARA—High Performance Computing, Forschungszentrum Jülich, D-52425 Jülich, Germany*

[9]*Department of Physics and Astronomy and HPC^2 Center for Computational Sciences, Mississippi State University, Mississippi State, Mississippi 39762, USA*

(Received 3 April 2017; published 1 December 2017)

Nuclear clustering describes the appearance of structures resembling smaller nuclei such as alpha particles (^{4}He nuclei) within the interior of a larger nucleus. In this Letter, we present lattice Monte Carlo calculations based on chiral effective field theory for the ground states of helium, beryllium, carbon, and oxygen isotopes. By computing model-independent measures that probe three- and four-nucleon correlations at short distances, we determine the shape of the alpha clusters and the entanglement of nucleons comprising each alpha cluster with the outside medium. We also introduce a new computational approach called the pinhole algorithm, which solves a long-standing deficiency of auxiliary-field Monte Carlo simulations in computing density correlations relative to the center of mass. We use the pinhole algorithm to determine the proton and neutron density distributions and the geometry of cluster correlations in ^{12}C, ^{14}C, and ^{16}C. The structural similarities among the carbon isotopes suggest that ^{14}C and ^{16}C have excitations analogous to the well-known Hoyle state resonance in ^{12}C.

DOI: 10.1103/PhysRevLett.119.222505

Nuclear clustering has been shown to be important in several well-known examples [1–4], however much remains to be discovered about the general nature of clustering in nuclei. There have been many exciting recent advances in *ab initio* nuclear structure theory [5–12] that link nuclear forces to nuclear structure in impressive agreement with experimental data. However, we still know very little about the quantum correlations among nucleons that give rise to nuclear clustering and collective behavior. The main difficulty in studying alpha clusters in nuclei is that the calculation must include four-nucleon correlations. Unfortunately, in many cases this dramatically increases the amount of computer memory and computing time needed in calculations of heavier nuclei. Nevertheless, there is promising work in progress using the symmetry-adapted no-core shell model [13], antisymmetrized molecular dynamics [14], fermionic molecular dynamics [15], the alpha-container model [16], the Monte Carlo shell model [17], and the Green's function Monte Carlo approach [18].

Lattice calculations using chiral effective field theory and auxiliary-field Monte Carlo methods have probed alpha clustering in the ^{12}C and ^{16}O systems [19–22]. However, these lattice simulations have encountered severe Monte Carlo sign oscillations in cases where the number of protons Z and number of neutrons N are different. In this Letter we solve this problem by using a new leading-order lattice action that retains a greater amount of symmetry, thereby removing nearly all of the Monte Carlo sign oscillations. The relevant symmetry is Wigner's SU(4) spin-isospin symmetry [23], where the four nucleon degrees of freedom can be rotated as four components of a complex vector. Previous attempts using SU(4) symmetry had failed due to the tendency of nuclei to overbind in larger nuclei. However, recent progress has uncovered important connections between local interactions and nuclear binding, as well as the significance of the alpha-alpha interaction [12,24,25]. Following this approach, we have constructed a leading-order lattice action with highly suppressed sign oscillations, which reproduces the ground-state binding energies of the hydrogen, helium, beryllium, carbon, and oxygen isotopes to an accuracy of 0.7 MeV per nucleon or better. The lattice results are shown in Fig. 1(a) in comparison with the observed ground state energies. The astonishingly good agreement at leading order in chiral effective field theory with only three free parameters is quite remarkable and

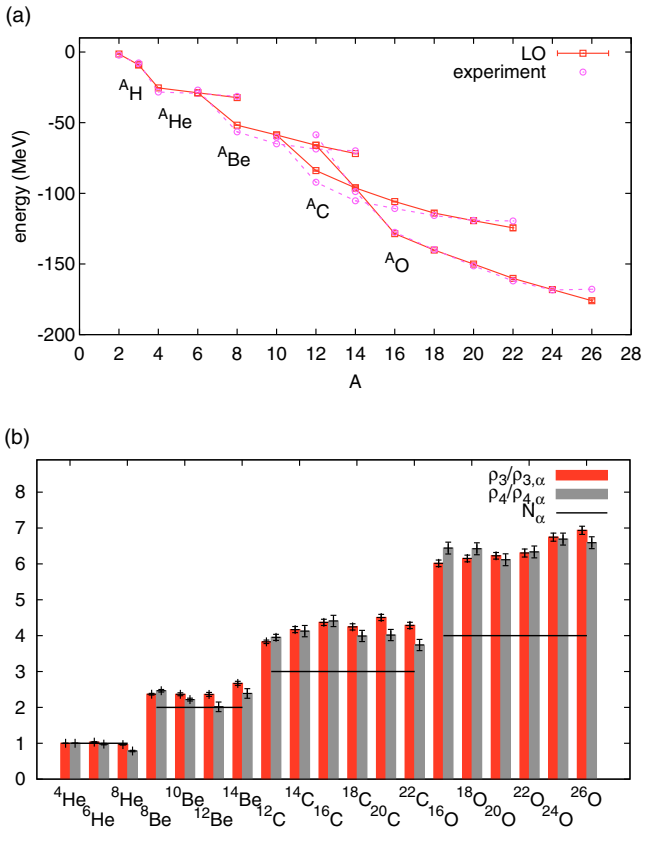

FIG. 1. In panel (a) we show the ground state energies versus number of nucleons A for the hydrogen, helium, beryllium, carbon, and oxygen isotopes. The errors are 1 standard deviation error bars associated with the stochastic errors and the extrapolation to an infinite number of time steps. In panel (b) we show $\rho_3/\rho_{3,\alpha}$ and $\rho_4/\rho_{4,\alpha}$ for the neutron-rich helium, beryllium, carbon, and oxygen isotopes. The error bars denote 1 standard deviation errors associated with the stochastic errors and the extrapolation to an infinite number of time steps. For comparison we show also the number of alpha clusters, N_α.

bodes well for future calculations at higher orders. We use auxiliary-field Monte Carlo simulations with a spatial lattice spacing of 1.97 fm and lattice time spacing 1.97 fm/c. We comment that the results for these ground state energies are equally good when including Coulomb repulsion and a slightly more attractive nucleon-nucleon short-range interaction. The full details of the lattice interaction, nucleon-nucleon phase shifts, simulation methods, and results are given in the Supplemental Material [26].

Let $\rho(\mathbf{n})$ be the total nucleon density operator on lattice site $\mathbf{n}$. We will use short-distance three- and four-nucleon operators as probes of the nuclear clusters. To construct a probe for alpha clusters, we define ρ_4 as the expectation value of $:\rho^4(\mathbf{n})/4!:$ summed over $\mathbf{n}$. The $::$ symbols indicate normal ordering where all annihilation operators are moved to the right and all creation operators are moved to the left. For nuclei with even Z and even N, there are likely no well-defined ^{3}H or ^{3}He clusters since their formation is not energetically favorable. Therefore, we can use short-distance three-nucleon operators as a second probe of alpha clusters. We define ρ_3 as the expectation value of $:\rho^3(\mathbf{n})/3!:$ summed over $\mathbf{n}$. A ^{3}H or ^{3}He cluster may form in nuclei with odd Z or odd N. In these cases we can use spin- and isospin-dependent three-nucleon operators to probe the ^{3}H and ^{3}He clusters. As we consider only nuclei with even Z and even N here, we focus on ρ_3 and ρ_4 for the remainder of the discussion. We note that another measure of clustering in nuclei by measuring short-distance correlations has been introduced in Ref. [27].

Because of divergences at short distances, ρ_3 and ρ_4 will depend on the short-distance regularization scale, which in our case is the lattice spacing. However, the regularization-scale dependence of ρ_3 and ρ_4 does not depend on the nucleus being considered. Therefore, if we let $\rho_{3,\alpha}$ and $\rho_{4,\alpha}$ be the corresponding values for the alpha particle, then the ratios $\rho_3/\rho_{3,\alpha}$ and $\rho_4/\rho_{4,\alpha}$ are free from short-distance divergences and are model-independent quantities up to contributions from higher-dimensional operators in an operator product expansion. The derivations of these statements are given in the Supplemental Material [26]. We have computed ρ_3 and ρ_4 for the helium, beryllium, carbon, and oxygen isotopes. As our leading-order interactions are invariant under an isospin mirror flip that interchanges protons and neutrons, we focus here on neutron-rich nuclei. The results for $\rho_3/\rho_{3,\alpha}$ and $\rho_4/\rho_{4,\alpha}$ are presented in Fig. 1(b). As we might expect, the values for $\rho_3/\rho_{3,\alpha}$ and $\rho_4/\rho_{4,\alpha}$ are roughly the same for the different neutron-rich isotopes of each element.

Since ρ_4 involves four nucleons, it couples to the center of the alpha cluster while ρ_3 gets a contribution from a wider portion of the alpha-cluster wave function. Therefore, a value larger than 1 for the ratio of $\rho_4/\rho_{4,\alpha}$ to $\rho_3/\rho_{3,\alpha}$ corresponds to a more compact alpha-cluster shape than in vacuum, and a value less than 1 corresponds to a more diffuse alpha-cluster shape. In Fig. 1(b) we observe that the ratio of $\rho_4/\rho_{4,\alpha}$ to $\rho_3/\rho_{3,\alpha}$ starts at 1 or slightly above 1 when N is comparable to Z, and the ratio gradually decreases as the number of neutrons is increased. This is evidence for the swelling of the alpha clusters as the system becomes saturated with excess neutrons. The effect has also been seen in ^{6}He and ^{8}He in Green's function Monte Carlo calculations [28].

We comment here that if one wants to study the swelling of alpha clusters in detail, then there are other local operators that provide more direct geometrical information such as the operators $:\rho^3(\mathbf{n})\rho(\mathbf{n}'):$ and $:\rho^2(\mathbf{n})\rho^2(\mathbf{n}'):$, where $\mathbf{n}'$ is a nearest-neighbor site to $\mathbf{n}$. These local operators have the advantage of measuring four-nucleon correlations directly rather than inferring them from the ratio of four-body and three-body correlations, which may not work well for cases with very large isospin imbalance.

The traditional approach to nuclear clustering usually involves a variational ansatz where the wave function is expanded in terms of some chosen set of alpha-cluster wave functions. However, the answer obtained this way may depend strongly on the details of the interactions and the choice of alpha-cluster wave functions. This problem of model dependence is solved by calculating short-range multinucleon quantities. Even though we use only short-range operators, the quantities $\rho_3/\rho_{3,\alpha}$ and $\rho_4/\rho_{4,\alpha}$ act as high-fidelity alpha-cluster detectors. Their values are strongly enhanced if the nuclear wave function has a well-defined alpha-cluster substructure. As shown in the Supplemental Material [26], the enhancement factor for $\rho_3/\rho_{3,\alpha}$ is $(R_A/R_\alpha)^6$, where R_A is the nuclear radius and R_α is the alpha-particle radius. The enhancement factor for $\rho_4/\rho_{4,\alpha}$ is an even larger factor of $(R_A/R_\alpha)^9$.

We denote the number of alpha clusters as N_α. A simple counting of protons gives $N_\alpha = 1$ for neutron-rich helium, $N_\alpha = 2$ for neutron-rich beryllium, $N_\alpha = 3$ for neutron-rich carbon, and $N_\alpha = 4$ for neutron-rich oxygen. However, the alpha clusters are immersed in a complex many-body system, and it is useful to quantify the entanglement of the nucleons comprising each alpha cluster with the outside medium. The observables $\rho_3/\rho_{3,\alpha}$ and $\rho_4/\rho_{4,\alpha}$ are useful for this purpose. Let us define $\delta_\alpha^{\rho_3}$ as the difference $\rho_3/\rho_{3,\alpha} - N_\alpha$ divided by N_α. Since $\delta_\alpha^{\rho_3}$ measures the deviation of the nuclear wave function from a pure product state of alpha clusters and excess nucleons, we call it the ρ_3 entanglement of the alpha clusters. In an analogous manner, we can also define the ρ_4 entanglement $\delta_\alpha^{\rho_4}$ as the difference $\rho_4/\rho_{4,\alpha} - N_\alpha$ divided by N_α. $\delta_\alpha^{\rho_4}$ turns out to be quantitatively similar to $\delta_\alpha^{\rho_3}$, though with more sensitivity to the shape of the alpha clusters.

In Fig. 1(b), we show N_α along with the ratios $\rho_3/\rho_{3,\alpha}$ and $\rho_4/\rho_{4,\alpha}$. The relative excess of $\rho_3/\rho_{3,\alpha}$ compared to N_α gives $\delta_\alpha^{\rho_3}$, and the relative excess of $\rho_4/\rho_{4,\alpha}$ compared to N_α gives $\delta_\alpha^{\rho_4}$. We see that $\delta_\alpha^{\rho_3}$ is negligible for ^{6}He and ^{8}He, indicating an almost pure product state of alpha clusters and excess neutrons. For the beryllium isotopes, $\delta_\alpha^{\rho_3}$ is about 0.18 for ^{8}Be and rises to about 0.34 for ^{14}Be. In this leading-order calculation the ^{8}Be ground state is about 1 MeV below the two-α threshold. The addition of the Coulomb interaction and other corrections should push this energy closer to threshold, and one expects $\delta_\alpha^{\rho_3}$ to decrease as a result. For the carbon isotopes, it is about 0.28 for ^{12}C and rises to a maximum of about 0.50 near the drip line. For the oxygen isotopes, $\delta_\alpha^{\rho_3}$ is about 0.50 for ^{16}O and increases with neutron number up to 0.73. For such high values of the ρ_3 entanglement, we expect a simple picture in terms of alpha clusters and excess neutrons will break down. $\delta_\alpha^{\rho_3}$ should be much lower for excited clusterlike states of the oxygen isotopes. With ρ_3 entanglement, we have a model-independent quantitative measure of nuclear cluster formation in terms of entanglement of the wave function. Our results show that the transition from clusterlike states in light systems to nuclear liquidlike states in heavier systems should not be viewed as a simple suppression of multinucleon short-distance correlations, but rather an increasing entanglement of the nucleons involved in the multinucleon correlations.

Despite the many computational advantages of auxiliary-field Monte Carlo methods, one fundamental deficiency is that the simulations involve quantum states that are superpositions of many different center-of-mass positions. Therefore, density distributions of the nucleons cannot be computed directly. To solve this problem we have developed a new method called the pinhole algorithm. In this algorithm an opaque screen is placed at the middle time step with pinholes bearing spin and isospin labels that allow nucleons with the corresponding spin and isospin to pass. We use A pinholes for a simulation of A nucleons, and the locations as well as the spin and isospin labels of the pinholes are updated by Monte Carlo importance sampling. From the simulations, we obtain the expectation value of the normal-ordered A-body density operator $:\rho_{i_1,j_1}(\mathbf{n}_1)\cdots\rho_{i_A,j_A}(\mathbf{n}_A):$, where $\rho_{i,j}$ is the density operator for a nucleon with spin i and isospin j.

Using the pinhole algorithm, we have computed the proton and neutron densities for the ground states of ^{12}C, ^{14}C, and ^{16}C. In order to account for the nonzero size of the nucleons, we have convolved the point-nucleon distributions with a Gaussian distribution with root-mean-square radius 0.84 fm, the charge radius of the proton [29,30]. The results are shown in Fig. 2 along with the experimentally observed proton densities for ^{12}C and ^{14}C [31], which we define as the charge density divided by the electric charge e. From Fig. 2 we see that the agreement between the calculated proton densities and experimental data for ^{12}C and ^{14}C is rather good. We show data for $L_t = 7, 9, 11, 13, 15$ time steps. The fact that the results have little dependence on L_t means that we are seeing ground state properties. As we increase the number of neutrons and go from ^{12}C to ^{16}C, the shape of the proton density profile remains roughly the same. However, there is a gradual decrease in the central density and a broadening of the proton density distribution. We see also that the excess neutrons in ^{14}C and ^{16}C are distributed fairly evenly, appearing in both the central region as well as the tail.

We now study the alpha-cluster structures of ^{12}C, ^{14}C, and ^{16}C in more detail. In order to probe the alpha cluster geometry, we use the fact that there is only one spin-up proton per alpha cluster. Using the pinhole algorithm, we consider the triangular shapes formed by the three spin-up protons in the carbon isotopes. This correlation function is free of short-distance divergences, and so, up to the contribution of higher-dimensional operators, it provides a model-independent measure that serves as a proxy for the geometry of the alpha-cluster configurations.

The three spin-up protons form the vertices of a triangle. When collecting the lattice simulation data, we rotate the triangle so that the longest side lies on the x axis. We also

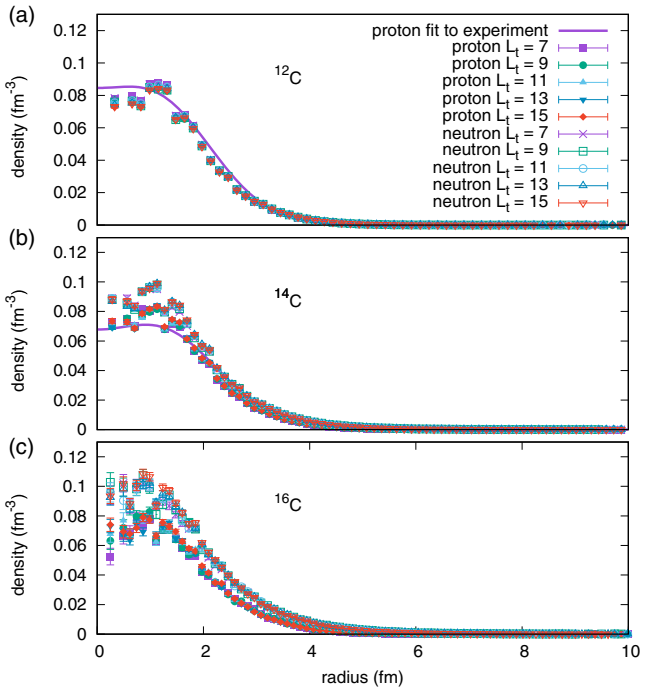

FIG. 2. Plots of the proton and neutron densities for the ground states of ^{12}C, ^{14}C, and ^{16}C vs radial distance. We show data for $L_t = 7, 9, 11, 13, 15$ time steps. We show ^{12}C in panel (a), ^{14}C in panel (b), and ^{16}C in panel (c). The errors are 1 standard deviation error bars associated with the stochastic errors. For comparison we show the experimentally observed proton densities for ^{12}C and ^{14}C [31].

rescale the triangle so the longest side has length 1, and flip the triangle, if needed, so that the third spin-up proton is in the upper half of the xy plane. Histograms of the third spin-up proton probability distributions for ^{12}C, ^{14}C, and ^{16}C are plotted in Figs. 3(a)–3(c) using the data at $L_t = 15$ time steps. The data for other values of L_t are almost identical. There is some jaggedness due to the discreteness of the lattice, but we see quite clearly that the histograms for ^{12}C, ^{14}C, and ^{16}C are very similar. While there is some increase in the overall radius of the nucleus, the rescaled cluster geometry of the three carbon isotopes remains largely the same. In each case we see that there is a strong preference for triangles where the largest angle is less than or equal to 90 deg. We should note that idea that the ground state of ^{12}C has an acute triangular alpha-cluster structure has a long history dating back to Ref. [32].

Given the rich cluster structure of the excited states of ^{12}C, this raises the interesting possibility of similar cluster states appearing in ^{14}C and ^{16}C. In particular, the bound 0_2^+ state at 6.59 MeV above the ground state of ^{14}C may be a bound-state analog to the Hoyle state resonance in ^{12}C at 7.65 MeV [33,34]. It may also have a clean experimental signature since low-lying neutron excitations are suppressed by the shell closure at eight neutrons. There is also a bound 0_2^+ in ^{16}C; however, in this case one expects

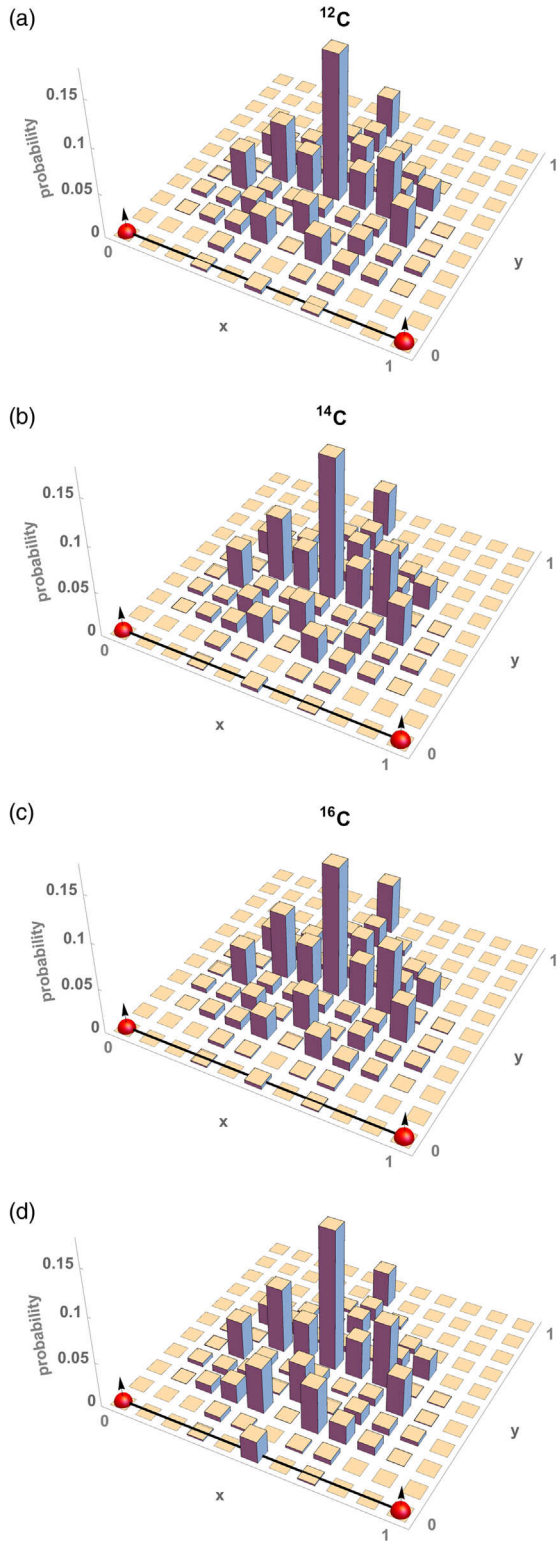

FIG. 3. The two red spheres with arrows indicate the first two spin-up protons, and the line connecting them is the longest side of the triangle. We show the third spin-up proton probability distribution in ^{12}C in panel (a), ^{14}C in panel (b), and ^{16}C in panel (c). The results are computed at $L_t = 15$ time steps. In panel (d) we show the third spin-up proton probability distribution for a simple Gaussian lattice model of the distribution of the spin-up protons.

low-lying two-neutron excitations to be important, thereby making the analysis more complicated. We note that there is ample experimental evidence for the cluster properties of the neutron-rich beryllium and carbon isotopes [35–38].

In order to analyze what we are seeing in the lattice data, we can make a simple Gaussian lattice model of the distribution of the spin-up protons. We consider a probability distribution $P(\mathbf{r}_1, \mathbf{r}_2, \mathbf{r}_3)$ on our lattice grid for the positions of the protons $\mathbf{r}_1$, $\mathbf{r}_2$, and $\mathbf{r}_3$. We take the probability distribution to be a product of Gaussians with root-mean-square radius 2.6 fm (charge radius of ^{14}C) and unit step functions that vanish if the magnitude of $\mathbf{r}_1 - \mathbf{r}_2$, $\mathbf{r}_2 - \mathbf{r}_3$, or $\mathbf{r}_3 - \mathbf{r}_1$, is smaller than 1.7 fm (charge radius of ^{4}He),

$$\exp\left(-\frac{\sum_i \mathbf{r}_i^2}{2(2.6\text{ fm})^2}\right)\prod_{j>k}\theta(|\mathbf{r}_j - \mathbf{r}_k| - 1.7\text{ fm}). \quad (1)$$

We can factor out the center-of-mass distribution of the three spin-up protons and recast the Gaussian factors as a product of Gaussians for the separation vectors $\mathbf{r}_1 - \mathbf{r}_2$, $\mathbf{r}_2 - \mathbf{r}_3$, or $\mathbf{r}_3 - \mathbf{r}_1$ with root-mean-square radius 4.5 fm,

$$\prod_{j>k}\exp\left(-\frac{(\mathbf{r}_j - \mathbf{r}_k)^2}{2(4.5\text{ fm})^2}\right)\theta(|\mathbf{r}_j - \mathbf{r}_k| - 1.7\text{ fm}). \quad (2)$$

In Fig. 3(d) we show the third spin-up proton probability distribution corresponding to this model. Despite the simplicity of this model with no free parameters, we note the good agreement with the lattice data for ^{12}C, ^{14}C, and ^{16}C. The only discrepancy is that the model overpredicts the probability of producing obtuse triangular configurations. This indicates that there are some additional correlations between the clusters that go beyond this simple Gaussian lattice model.

In this Letter we have presented a number of novel approaches to computing and quantifying clustering and entanglement in nuclei. We hope that this work may help to accelerate progress in theoretical and experimental efforts to understand the correlations that produce nuclear clustering and collective behavior.

We are grateful for the hospitality of the Kavli Institute for Theoretical Physics at U.C. Santa Barbara for hosting E. E., H. K., and D. L. We are indebted to Ingo Sick for providing the experimental data tables on the electric form factor for ^{12}C. We acknowledge partial financial support from the CRC110: Deutsche Forschungsgemeinschaft (SFB/TR 110, "Symmetries and the Emergence of Structure in QCD"), the BMBF (Verbundprojekt 05P2015—NUSTAR R&D), the U.S. Department of Energy (Grant No. DE-FG02-03ER41260), and U.S. National Science Foundation Grant No. PHY-1307453. Further support was provided by the Magnus Ehrnrooth Foundation of the Finnish Society of Sciences and Letters and Chinese Academy of Sciences (CAS) President's International Fellowship Initiative (PIFI) Grant No. 2017VMA0025. The computational resources were provided by the Jülich Supercomputing Centre at Forschungszentrum Jülich, RWTH Aachen, and North Carolina State University.

[1] K. I. H. Horiuchi and K. Kato, Prog. Theor. Phys. Suppl. **192**, 1 (2012).
[2] *Clusters in Nuclei*, Lecture Notes in Physics, Vol. 3, edited by C. Beck (Springer-Verlag, Berlin 2014).
[3] Y. Funaki, H. Horiuchi, and A. Tohsaki, Prog. Part. Nucl. Phys. **82**, 78 (2015).
[4] M. Freer, H. Horiuchi, Y. Kanada-En'yo, D. Lee, and U.-G. Meißner, arXiv:1705.06192.
[5] C. Romero-Redondo, S. Quaglioni, P. Navratil, and G. Hupin, Phys. Rev. Lett. **113**, 032503 (2014).
[6] P. Maris, J. P. Vary, A. Calci, J. Langhammer, S. Binder, and R. Roth, Phys. Rev. C **90**, 014314 (2014).
[7] T. Dytrych, P. Maris, K. D. Launey, J. P. Draayer, J. P. Vary, D. Langr, E. Saule, M. A. Caprio, U. Catalyurek, and M. Sosonkina, Comput. Phys. Commun. **207**, 202 (2016).
[8] T. Duguet, V. Soma, S. Lecluse, C. Barbieri, and P. Navratil, Phys. Rev. C **95**, 034319 (2017).
[9] S. R. Stroberg, A. Calci, H. Hergert, J. D. Holt, S. K. Bogner, R. Roth, and A. Schwenk, Phys. Rev. Lett. **118**, 032502 (2017).
[10] R. F. Garcia Ruiz *et al.*, Nat. Phys. **12**, 594 (2016).
[11] G. Hagen, G. R. Jansen, and T. Papenbrock, Phys. Rev. Lett. **117**, 172501 (2016).
[12] S. Elhatisari, N. Li, A. Rokash, J. M. Alarcon, D. Du, N. Klein, B. N. Lu, Ulf-G. Meißner, E. Epelbaum, H. Krebs, T. A. Lähde, D. Lee, and G. Rupak, Phys. Rev. Lett. **117**, 132501 (2016).
[13] K. D. Launey, T. Dytrych, and J. P. Draayer, Prog. Part. Nucl. Phys. **89**, 101 (2016).
[14] Y. Yoshida and Y. Kanada-En'yo, arXiv:1609.01407.
[15] H. Feldmeier and T. Neff, arXiv:1612.02602.
[16] P. Schuck, Y. Funaki, H. Horiuchi, G. Roepke, A. Tohsaki, and T. Yamada, Phys. Scr. **91**, 123001 (2016).
[17] T. Yoshida, N. Shimizu, T. Abe, and T. Otsuka, J. Phys. Conf. Ser. **569**, 012063 (2014).
[18] A. Lovato, S. Gandolfi, J. Carlson, S. C. Pieper, and R. Schiavilla, Phys. Rev. Lett. **117**, 082501 (2016).
[19] E. Epelbaum, H. Krebs, D. Lee, and Ulf-G. Meißner, Phys. Rev. Lett. **106**, 192501 (2011).
[20] E. Epelbaum, H. Krebs, T. A. Lähde, D. Lee, and Ulf-G. Meißner, Phys. Rev. Lett. **109**, 252501 (2012).
[21] E. Epelbaum, H. Krebs, T. A. Lähde, D. Lee, and Ulf-G. Meißner, Phys. Rev. Lett. **110**, 112502 (2013).
[22] E. Epelbaum, H. Krebs, T. A. Lähde, D. Lee, Ulf-G. Meißner, and G. Rupak, Phys. Rev. Lett. **112**, 102501 (2014).
[23] E. Wigner, Phys. Rev. **51**, 106 (1937).
[24] S. Elhatisari, D. Lee, G. Rupak, E. Epelbaum, H. Krebs, T. A. Lähde, T. Luu, and U.-G. Meißner, Nature (London) **528**, 111 (2015).

[25] A. Rokash, E. Epelbaum, H. Krebs, and D. Lee, Phys. Rev. Lett. **118**, 232502 (2017).
[26] See Supplemental Material at http://link.aps.org/supplemental/10.1103/PhysRevLett.119.222505 for a discussion of the lattice interactions, scattering data, and computational methods.
[27] C. L. Zhang, B. Schuetrumpf, and W. Nazarewicz, Phys. Rev. C **94**, 064323 (2016).
[28] R. B. Wiringa, S. C. Pieper, J. Carlson, and V. R. Pandharipande, Phys. Rev. C **62**, 014001 (2000).
[29] M. A. Belushkin, H.-W. Hammer, and Ulf-G. Meißner, Phys. Rev. C **75**, 035202 (2007).
[30] R. Pohl *et al.*, Nature (London) **466**, 213 (2010).
[31] F. J. Kline, H. Crannell, J. T. O' Brien, J. McCarthy, and R. R. Whitney, Nucl. Phys. **A209**, 381 (1973).
[32] L. R. Hafstad and E. Teller, Phys. Rev. **54**, 681 (1938).
[33] F. Hoyle, Astrophys. J. Suppl. Ser. **1**, 121 (1954).
[34] C. Cook, W. A. Fowler, C. C. Lauritsen, and T. Lauritsen, Phys. Rev. **107**, 508 (1957).
[35] H. G. Bohlen, T. Dorsch, T. Kokalova, W. von Oertzen, C. Schulz, and C. Wheldon, Nucl. Phys. **A787**, 451 (2007).
[36] H. G. Bohlen *et al.*, Nucl. Phys. **A722**, C3 (2003).
[37] M. Freer, AIP Conf. Proc. **1072**, 58 (2008).
[38] D. J. Marin-Lambarri, R. Bijker, M. Freer, M. Gai, T. Kokalova, D. J. Parker, and C. Wheldon, Phys. Rev. Lett. **113**, 012502 (2014).